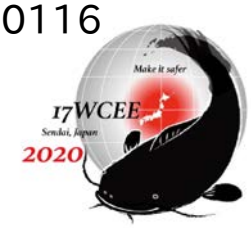

17th World Conference on Earthquake Engineering, 17WCEE
Sendai, Japan - September 13th to 18th 2020

INFLUENCE OF CENTRAL OPENINGS AT THE BASE IN FLEXURAL RC WALLS

G. Muñoz-Arriagada[(1)], L. Massone[(2)], F. Rojas[(3)]

[(1)] *Ph.D. Candidate, University of Auckland, garr548@aucklanduni.ac.nz*
[(2)] *Associate professor, University of Chile, lmassone@uchile.cl*
[(3)] *Assistant professor, University of Chile, fabianrojas@uchile.cl*

Abstract

Reinforced Concrete (RC) walls usually represent the main component in the lateral resistant system of residential buildings in Chile. The common practice considers complex geometries and discontinuities in height, mainly in the first story. Many of these elements were severely damaged after the 2010 Mw 8.8 Maule earthquake. Recent research demonstrates that flexural dominant RC walls with setback discontinuities had a detrimental performance because the irregularity limits the plastic hinge length. However, the Chilean code does not provide special provisions for any discontinuities in RC walls, similar to many design codes elsewhere. The results of an experimental and numerical study of RC walls with a central opening at the base is summarized. Four 2.6 m height, 0.9 m length and 0.15 m thick walls were constructed with different shapes of the opening (15% and 30% of the length, and 11% and 22% of the wall height). The specimens were tested under constant axial load and increasing cyclic lateral displacements. One of the specimens has two slab elements at the base. Results indicate that lateral strength is similar in all cases, but the opening had a detrimental effect on the displacement capacity. Besides, this effect varies with opening size, being the width of the opening more influential than the height. The specimen with a wider and taller opening had a 30% reduction in the displacement capacity. Numerical analysis was done through a finite element modeling using flexural and shear-flexural models. The results show that the influence of the opening affects the vertical compressive strain in the boundary element near the base of the wall. Distribution of the curvature in height and local behavior in the piers generated by the opening are studied. Monotonic analysis (pushover) are also used to represent the behavior of walls with central openings, indicating that the increase of concrete compression strain at wall boundary can only be captured with the incorporation of longitudinal bar buckling and a pre-cycle that triggers its buckling behavior. Thus, modeling suggestions are discussed that provide consistent results with the experimental observations.

Keywords: walls; experimental; discontinuities, strain, flexural

1. Introduction

The 2010 Mw 8.8 Maule earthquake has been the biggest earthquake occurred in the last decade in Chile, testing the Chilean seismic design across the country. Reinforced concrete (RC) structures had a good overall performance, however, several modern buildings showed damage in structural walls, which are the main element used to resist earthquake demands in Chilean residential buildings. The observed damage in these elements includes concrete crushing, longitudinal reinforcement buckling, longitudinal reinforcement fracture, and both global and local instability failures. Different studies after the earthquake attributed the main reasons of these failures to the lack of confinement requirements in the boundary elements [1], the presence of discontinuities, and high axial load forces [2, 3]. The absence of confined boundary elements was due to a relaxation in the Chilean building code, already modified in the actual RC design code. The high presence of discontinuities in the wall height is due to architectural requirements since generally the first floor and the first underground had a different use compared to the upper floors, requiring entrances and doors in these levels. Fig. 1 (a) shows a wall elevation with irregular openings in the first floor, and Fig. 1 (b), Fig. 1 (c), and Fig. 1 (d) show the damaged zone highlighted in Fig. 1 (a) [4].

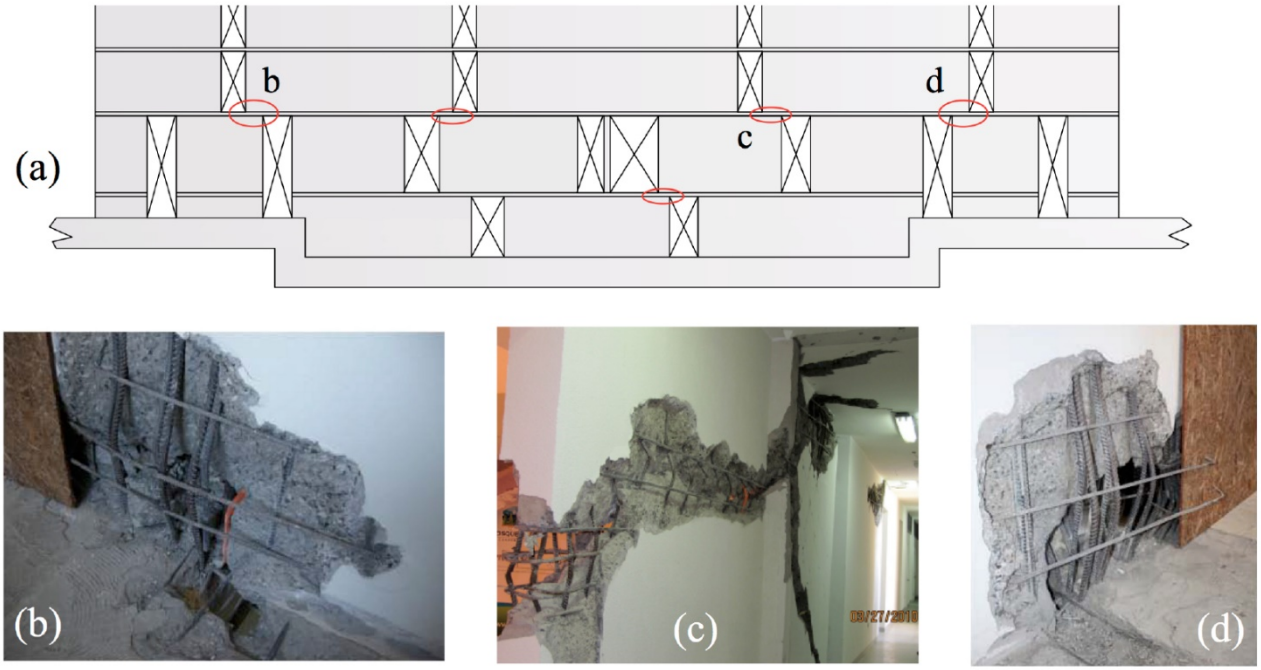

Fig. 1 - (a) Elevation view of a Chilean building damaged in the 2010 earthquake, (b), (c), and (d) Damage highlighted in (a).

Despite the high use of RC walls in high-rise buildings, there is a modest amount of experimental research that considered discontinuities in walls. Taylor et al. [5] tested scaled walls to show whether that displacement-based design is valid for walls with discontinuities, studying two quarter-scale walls. Results show that slender walls with an opening at the base can have good displacement capacity, as long as detailing is designed under a displacement-based approach. Although results indicate that target displacements can be achieved, there is no studies of the limitation of the displacement approach, or the impact of different opening size in walls. Ali and Wight [6] tested four scaled RC (reinforced concrete) walls: three with staggered openings and one with no openings. The objective was to study the influence of the location of the openings. Results reveal that all specimens with openings show stable behavior and large displacement capacity, although with smaller ductility than the specimen without openings. According to Ali and Wight, the staggered opening configuration resulted in a better option than “in line” openings, similar to coupled walls, because less detailing near the openings is required. Similar to the results by Taylor et al., strength degradation was observed in the smaller wall pier at the base (smaller wall formed by the presence of the opening at the base) and controlled

by the boundary detailing. Mosoarca [7] tested 5 specimens, with 4 of them with a similar configuration as the walls tests by Ali and Wight (3 staggered walls and a solid wall), and a fifth specimen that considered aligned openings placed at the center of the wall. The presence of openings reduced the displacement capacity of the walls, but it was the specimen with aligned openings the one that presented the least ductility.

In the Chilean RC design code, that follows mainly the ACI 318-08 code, the detailing verification of slender walls is based on a displacement- based approach, which assumes a model of plastic hinge at the wall base that defines the transverse boundary reinforcement requirements. However, the formulation of detailing is commonly based on a rectangular wall without any discontinuity. Considering the previous, this paper shows the results of an experimental and numerical study of four slender reinforced concrete walls with different opening characteristics at the base to determine the influence of a central discontinuity in the wall behavior, as well as the presence of slabs.

2. Description of the experimental program

2.1 Materials

The concrete average compressive strength was 39.6 MPa for specimens MR1, MR2 and MR3, and 41.2 MPa for specimen MR4. The yield stress of the steel reached an average value of 490 MPa. W1 has a compressive strength of 33.2 MPa and an average yield stress of 490 MPa. Walls were built with materials properties and steel qualities typical of medium and high-rise buildings in Chile, as it is indicated by Estay [8].

2.2 Walls description

Four RC walls were designed and constructed with a central opening at the base using common characteristics in Chilean construction. The overall dimensions are 2650 mm high, 900 mm long and 150 mm thick. The specimens were differentiated by its opening size and the presence/absence of a slab. MR1 has a discontinuity of 135 mm long by 300 mm high, being the smallest in the project. In MR2, the opening is 270 mm long and 300 mm high, having the same height and twice the length of MR1. MR3 increases twice the height and the length stays as same as for MR2 having a 270 mm by 600 mm discontinuity. MR4 has the same opening as MR3, but with two slabs of 600 mm by 900 mm by 65 mm centered located at 300 mm and 600 mm measured from the base of the wall. The general dimensions are identical to those of Massone et al. [9] to compare the results to a base or common wall, W1 (here referred as MR0), which can be seen in Fig. 2.

The longitudinal reinforcement consists of 4 bars ϕ16 located at each boundary, confined with ϕ6 stirrups spaced every 70 mm until 900 mm from the beginning of the wall; then one side has no stirrups and the other one has ϕ6 stirrups spaced every 100 mm until the top of the wall. The longitudinal reinforcement at each edge of the discontinuity (opening) includes 2ϕ10 bars. The horizontal reinforcing bars consist of ϕ8 bars spaced at 200 mm in the vertical direction, decreasing the spacing in the opening in order to achieve a similar shear strength as in the continuous wall. Vertical distributed reinforcement bars were 4 ϕ8 bars above the opening. Vertical and horizontal reinforcement are doubled at the top of the wall to ensure proper load transfer. Roughly, reinforcement quantity and layout, dimensions and material properties were selected to recall wall W1 (MR0) design for comparison purposes. The slabs in MR4 are reinforced with 3ϕ8 bars in each side (superior and inferior) perpendicular to the wall and 4ϕ8 bars in each side parallel to the wall, where two of them (for each side) are in plane with the wall. The four tested walls and the base wall are depicted in Fig. 2.

2.3 Instrumentation and data acquisition

In all specimens, three types of devices are used to record the experimental data. About 15 strain gages are located on the reinforcing bars of each specimen in web horizontal bars near the discontinuity, boundary longitudinal bars and longitudinal bars at the side of opening. On one side of the wall around 30 LVDT's were installed, measuring top lateral wall displacement, internal flexural and shear deformations, besides of sensors located in the pedestal of the specimen recording possible sliding or rigid body rotations. On the other side of the walls, a photogrammetry system is implemented, as an alternative of the use of LVDT.

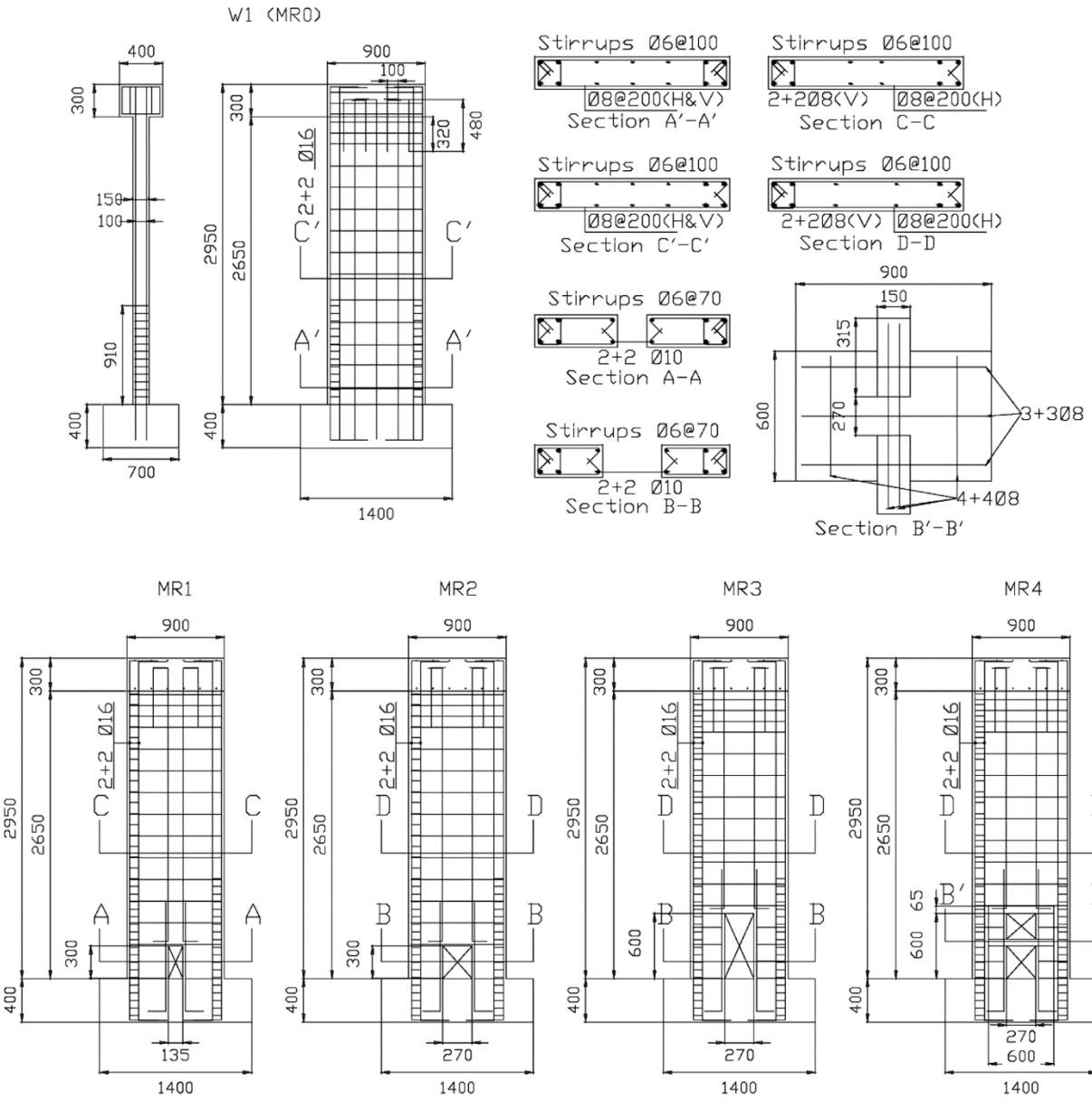

Fig. 2 - Walls geometry and reinforcement (units in mm).

2.4 Test Setup and loading protocol

Each specimen was anchored to a strong floor using posttensioned rods in the pedestal. A constant axial load of roughly 0.07f'cAg (Ag, wall gross cross-section) is applied by means of hydraulic jacks located on the top of the load transfer system. A hydraulic actuator attached to the reaction wall at 2.8m from the base of the wall applies the required lateral displacement. In terms of drift values, these are 0.1%, 0.2%, 0.3%, 0.4%, 0.6%, 0.9%, 1.35%, 2%, 3% and 4% of the height. Three cycles are performed for each drift level. A steel frame is attached to the strong floor and uses four struts to secure out of plane stability in the wall. Fig. 3 shows the final assembly before the test, and a general schematic of the test setup.

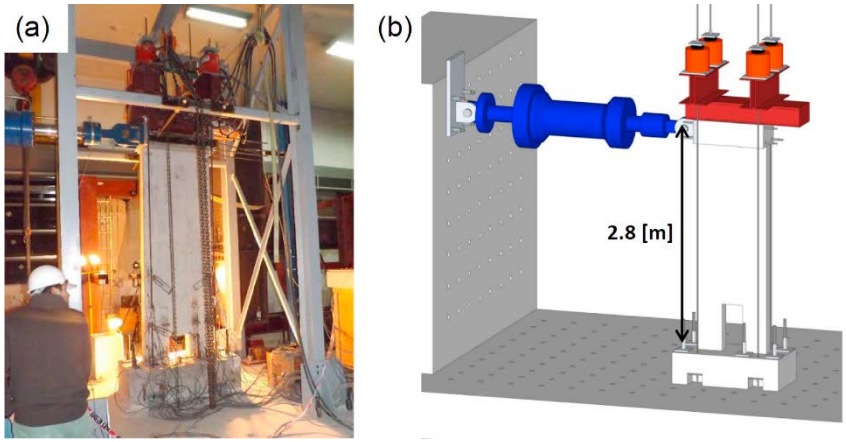

Fig. 3 - (a) Test setup, (b) General scheme (Out of plane system removed for clarity).

3. Experimental results

3.1 Overall Behavior

All specimens have a similar behavior for the first drift levels, having horizontal cracks at the base and diagonal cracks distributed in height starting from a drift of 0.3%. Cracks, in general, are clearly visible at 0.6% drift.

For specimen MR1, at the second 3% drift cycle in negative direction there is concrete cover loss at wall boundary. In the negative direction of the third 4% drift there is compression failure in the boundary wall, with local buckling of the boundary reinforcement bar and the rebar located at the opening. Finally, in the positive direction of the third 4% drift takes place a compression failure, with buckling of the boundary reinforced bar and the rebar located at the opening. Final configuration can be seen in Fig. 4(a).

Specimen MR2 does not show remarkable cracks until first 3% drift cycle. At that level (positive direction), there is a sudden concrete cover loss, besides of a shear crack (Fig. 4b). Failure occurs in the second 3% drift level in negative direction, with concrete cover loss in the inner face of the opening, together with concrete spalling and buckling of bars located at the boundary and opening edge (Fig. 4b).

In specimen MR3 during the first 3% drift cycle in the negative direction, a vertical crack appears near the inner face of the opening. The concrete cover loss happens in the first 3% drift cycle in positive direction, together with buckling of bars located at the boundary and opening edge. A notorious shear crack appears in one leg (side of the opening) of the wall, at the height of the opening. Finally, failure occurs in the second 3% drift cycle in the negative direction, with a brittle shear crack, similar to the other side of the opening (Fig. 4c).

The presence of slabs in MR4 makes a concentration of cracks below the second slab. The concrete cover loss happens in the first 2% drift cycle in the negative direction in the compressed boundary side, and during the second 3% drift cycle in the negative direction in the other compressed boundary side. At the second 2% drift cycle in the negative direction cracks can be seen in the first slab, coupling the two parts of the wall. In the second 3% drift cycle in the negative direction failure is reached with the presence of a shear crack, together with buckling of longitudinal bars (Fig. 4d).

Except in the negative direction of MR1, in all cases a predominant diagonal crack formed from the top corner of the opening up to the wall edge at the base. However, the boundary element crushed at the base of the crack, triggered by the flexural and shear demands in the region. The buckling of the longitudinal reinforcement in the boundary element and in the opening edge also confirmed the high flexural demands in the pier. Then, even with the predominant diagonal crack, the strength drop was triggered by concrete crushing in the boundary element at the wall base and buckling of the longitudinal reinforcement at the boundary.

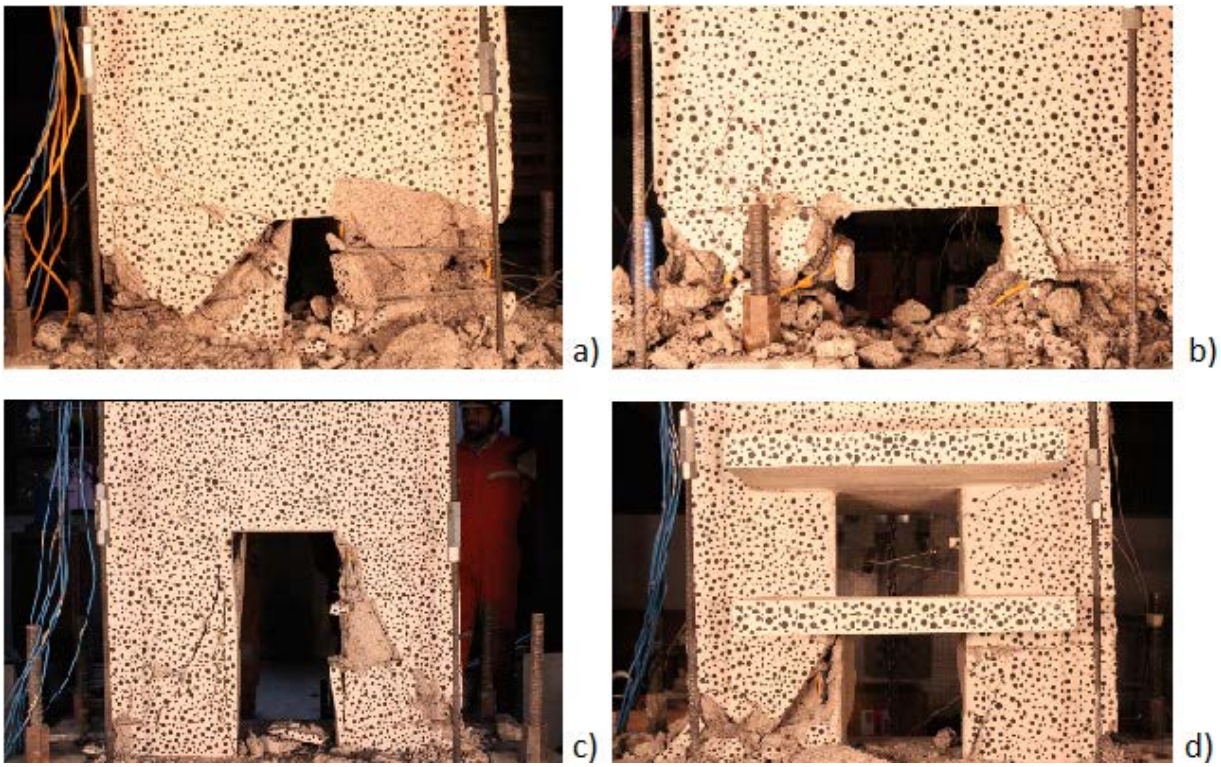

Fig. 4 - Damage at wall base for specimens: (a) MR1, (b) MR2, (c) MR3 and (d) MR4.

3.2 Load versus displacement response

The lateral displacement (corrected by pedestal sliding and rotation) versus lateral load is shown in Fig. 5 for all specimens. The blue line shows the results for each wall, while grey line represented the results for W1, where can be seen stable behavior up to 4.0% drift (first important degradation). Overall results indicate that all specimens reach almost the same lateral strength, because yielding is achieved in flexure, as designed, where capacity is largely influenced by the boundary flexural reinforcement. The main difference is the displacement capacity reached by the specimens. Results of MR1 are shown in Fig. 5(a), where stable behavior can be seen until last 4% drift cycle. Stiffness is similar in both loading directions, but there is a small difference in the lateral strength close to 5%. Sudden degradation occurs close to 4% drift while trying to reach 6% drift (the corrected maximum drift achieved – before a lateral force drop of 20% - was about 3.7%). The overall response is quite similar to the specimen without opening (grey line in Fig. 5). The larger (longer) opening in the specimen MR2 reduces considerably the displacement capacity (Fig. 5b). Both strength and stiffness are symmetric in each loading direction and similar to MR1. While reaching the first 3% drift cycle in the positive direction, degradation is observed (the corrected maximum drift achieved was about 2.6%). Fig. 5(c) shows the response of specimen MR3. Similar to the other cases, stiffness and strength are symmetric and similar to MR1 and MR2. There is no great difference between MR3 and MR2. Failure is reached when trying to reach the second cycle of 3% drift in the negative direction; although degradation was already observed in the previous cycle (the corrected maximum drift achieved was about 2.6%). MR4 response is shown in Fig. 5(d). Like the other specimens, strength and stiffness are symmetric and similar to the other walls. Nevertheless, there is a big improvement in the deformation capacity compared with the specimen without slab and the same opening size (MR3), but not as well as specimen MR1. Slabs allow finishing all three 3% drift cycles, having the wall a brittle failure trying to reach 4% (the corrected maximum drift achieved was about 3.2 %).

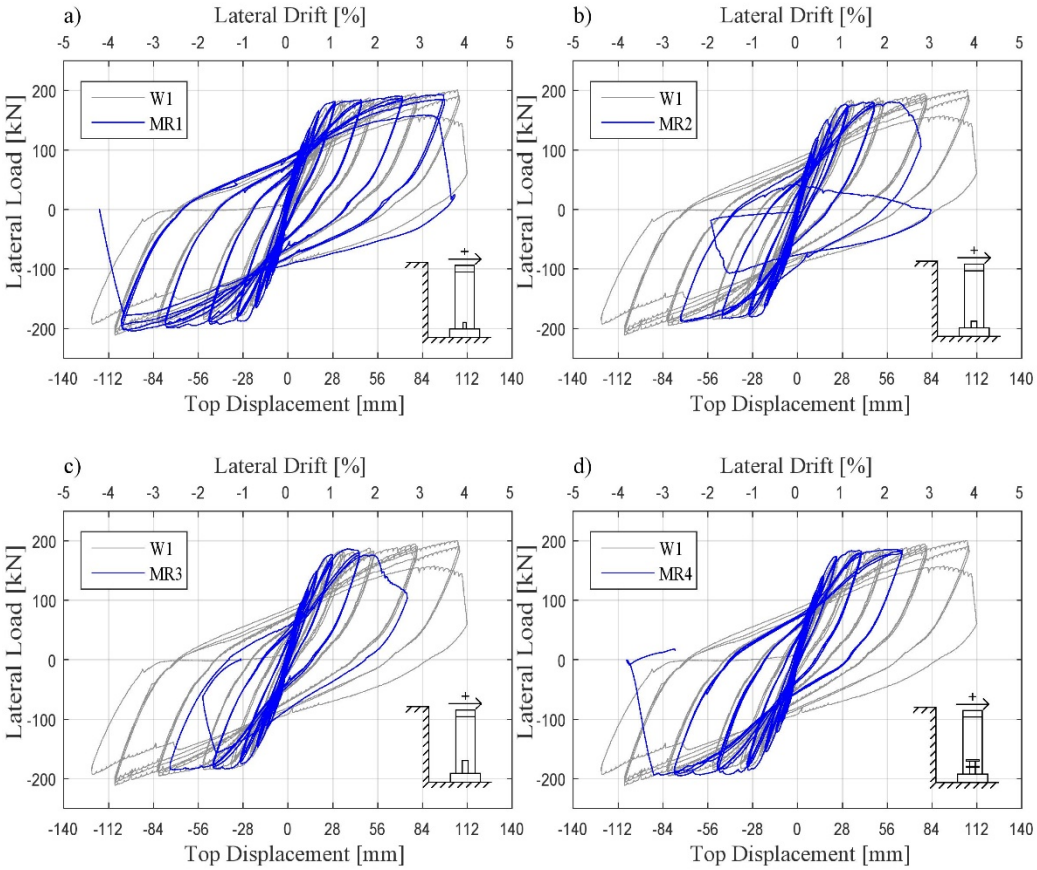

Fig. 5 - Load versus displacement response of specimen – (a) MR1, (b) MR2, (c) MR3 and (d) MR4.

4. Numerical models

4.1. Finite element model formulation

A finite element modeling was performed using the SAFE program implemented by Rojas [10] and extended by Rojas et al. [11, 12]. Rectangular membrane-type and shell-type elements are used, with four nodes and three degrees of freedom (two displacements and one rotation) for the membranes [11], and six degrees of freedom (three displacements and three rotations) for the shells [12]. The elements are constituted by concrete and steel layers. For the concrete layers, an orthotropic average model formulation with a rotating-angle approach is used, represented by uniaxial constitutive models in each principal direction. For the steel layer, which is fully bonded with concrete, the material constitutive model uses a uniaxial average stress-strain relationship of steel bars embedded in concrete. Two different models are used to represent the uniaxial constitutive model for the steel: one does not consider the buckling in the formulation [13], and the other that is used to represent the behavior of the longitudinal bars at the wall edges that are susceptible of buckling [13]. For all models, the discretization distinguishes between confined and unconfined concrete (Fig. 6a), as well as, the steel reinforcement in the section. In the case of boundary reinforcement (ϕ16), buckling is restricted and therefore the model with buckling almost does not change the original response (Fig. 6b), whereas for distributed reinforcement (ϕ10) buckling changes the response (Fig. 6c). Two types of models are considered for analysis. The complete model considers the implementation of the finite element formulation, which by definition includes bending and shear behavior (F+S). The flexural model is based on the complete model but imposes the Bernoulli hypothesis (F) by placing rigid horizontal elements, discontinuous at the opening, at every level.

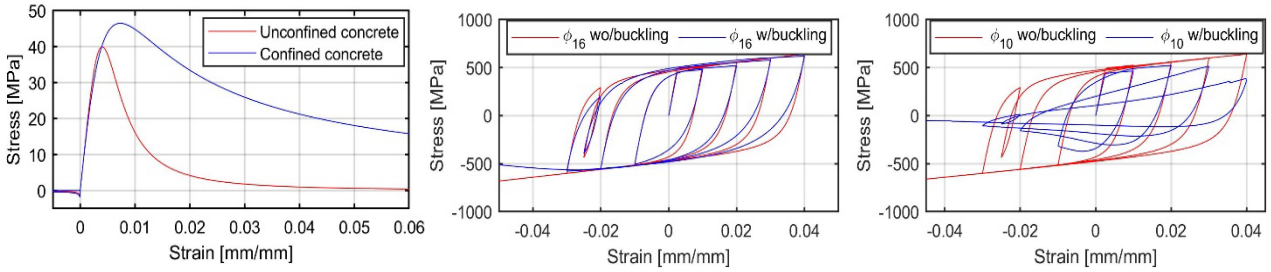

(a) (b) (c)

Fig. 6 - Constitutive laws (a) Concrete, (b) Boundary reinforcement, and (c) Opening reinforcement.

4.2. Load versus displacement response

Fig. 7 shows the results obtained by the model, where the red color corresponds to the complete model and the blue color the pure bending model. As a reference, the gray color shows the experimental results of the corresponding wall. In general, it can be seen that the models are capable of accurately reflecting stiffness, strength and displacement capacity. Considering as a relevant parameter the maximum drift reached by the walls, it is shown that, while the modeling that considers both bending and shear is more precise than the flexural, the latter is still able to capture the overall behavior of the walls in strength, stiffness and displacement capacity.

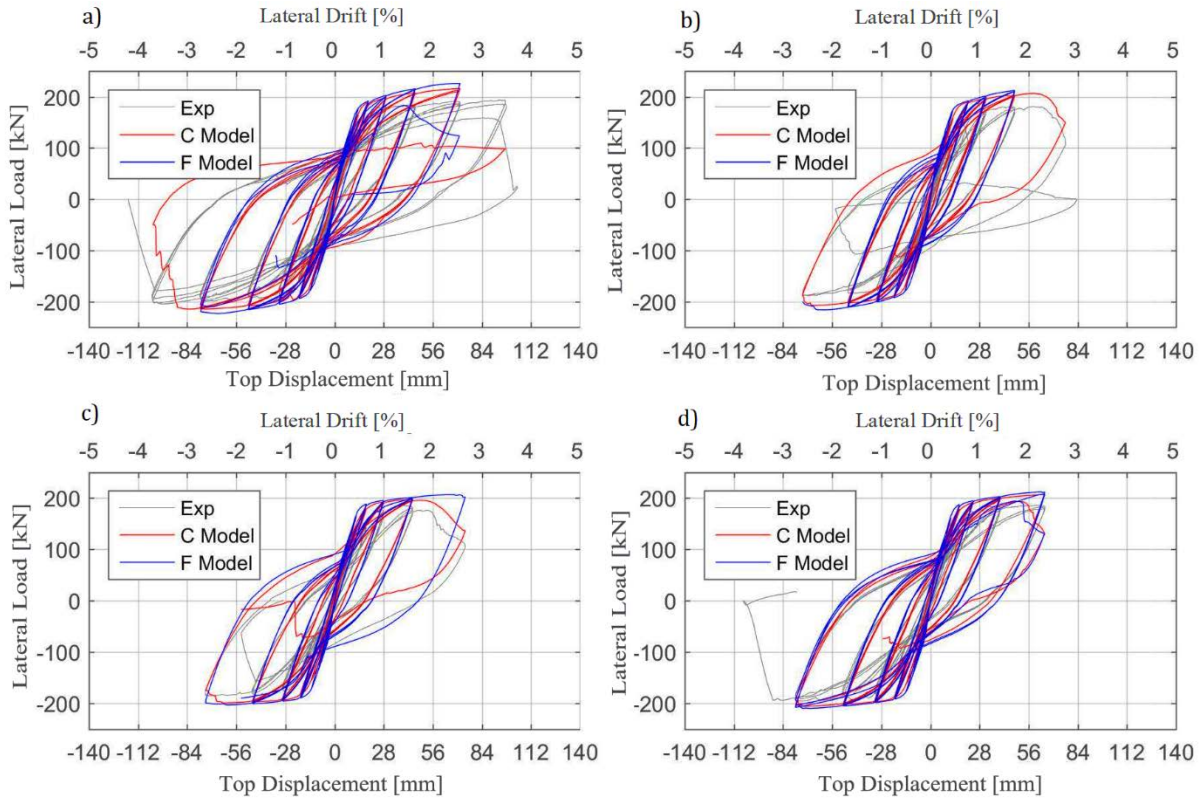

Fig. 7 - Load versus displacement response of the specimen: (a) MR1, (b) MR2, (c) MR3, and (d) MR4 (blue flexural mode, red complete model and gray experimental results).

4.2. Compressive strain at boundary elements

The failure of the walls (except MR1 in the negative direction) was triggered by concrete crushing and bar buckling of the longitudinal reinforcement. To understand the demands in the boundary element at the wall base, the average compressive (vertical) deformation versus the drift level is plotted in Fig. 8(a) using the zone

of maximum compression shown in Fig. 8(b) that represent the model discretization. There is a correlation between this value and the order of failure recorded in the walls: from MR0 with the highest recorded drift, and then MR1, MR4, MR2, to MR3 with the lowest reached displacement. Thus, the influence of the openings in the drift capacity could be used for wall boundary detailing, given that compression strain is a parameter normally used in detailing.

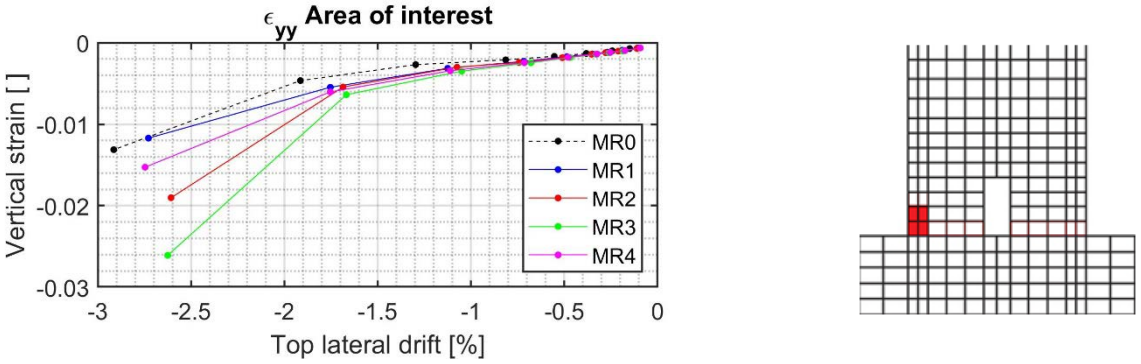

Fig. 8 - (a) Compressive strain, and (b) Area of interest.

4.2. Monotonic analysis

Two monotonic analysis of the walls were conducted to obtain the average compressive strain in the area of interest previously defined. The first case started from the origin and was pulled up to 3% in the positive direction, while the second case was pushed up to 2% in the other direction first. The results are presented in Fig 9(a) and Fig 9(b), respectively. In the case without previous loading the strain values are almost identical up to 2%, which does not correlate with the results shown in Fig. 8. Moreover, after this point the values does not correlate with the observed order of failure of the walls. The pre loading applied in the second analysis is enough to separate the responses and to correlate them with the previous results (except for MR2), although the differences are lesser than the observed in Fig. 8. The preloading triggers the differences in the behavior of the reinforcement affected by buckling, and the pure monotonic case is not able to capture it. Thus, the loading protocol with three cycles per drift level accentuate even more the influence of buckling in the reinforcement. Concrete degradation in cyclic loading also contributes to increase the differences between the cyclic and monotonic results.

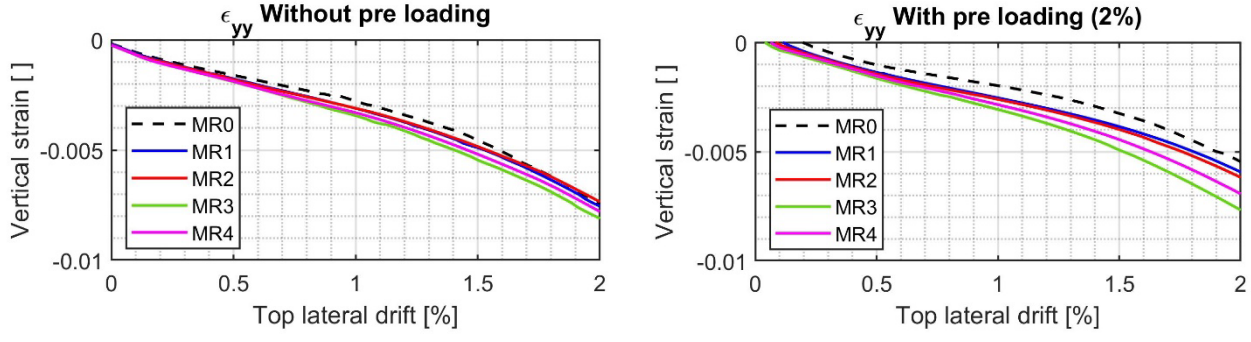

Fig. 9 – Compressive strain analysis: (a) Monotonic loading, (b) Monotonic loading after pushing up to 2% in the other direction.

5. Conclusions

This paper summarizes the experimental study of four scaled slender RC walls with central opening at the base. Four specimens are constructed and tested in cantilever with a cyclic lateral point load at the wall top. A constant axial load was also considered (~0.07f'cAg). One of the specimens has two centered slabs near the base. Walls are designed to have the same flexural strength, which is confirmed with the test results. The main global difference is the deformation capacity, being reduced with the size of the opening. Comparison between MR1 and MR2 and between MR2 and MR3 reveals that opening width is more influential than height in the displacement capacity. Since the influence of the openings affects the deformation capacity and not strength, proposals for design improvement should be focused on detailing. The use of slabs has a remarkable influence in the wall response: despite having a taller opening, MR4 has a similar behavior as MR2 (with the same opening width, but half the opening height compared to MR4). This suggests that experimental and analytical studies should consider the slab impact in discontinuous walls. The finite element model was able to represent the global behavior of the tested walls. Complete models and pure bending models capture the response of the walls, being slightly more accurate the complete model. Thus, the pure bending model of walls with openings is considered adequate to capture stiffness, strength and displacement capacity. Monotonic analysis conducted in the walls showed the influence of cyclic damage in the compressive vertical strain at the boundary element, where damage concentrated. As the flexural cyclic analysis done for the walls were able to capture the overall response, the modelling of the walls considering buckling of the reinforcement becomes crucial to achieve accurate results.

6. Acknowledgments

This work was financially supported by FONDECYT regular 2013N°1130219 "Analytical and experimental study of RC walls with discontinuities". Also, the help with the testing by Jorge Rivas, Ernesto Inzunza, Victor González, Pedro Soto, Sebastian Diaz and Ignacio Manriquez is also thanked.

7. References

[1] Welt TS, Massone LM, LaFave JM, Lehman DE, McCabe SL, Polanco P. Confinement behavior of rectangular reinforced concrete prisms simulating wall boundary elements. J Struct Eng-ASCE 2017;143(4):04016204.

[2] Wallace JW, Massone LM, Bonelli P, Dragovich J, Lagos R, Lüders C, et al. Damage and implications for seismic design of rc structural wall buildings. Earthquake Spectra 2012;28(S1):S281–99.

[3] Massone LM, Bonelli P, Lagos R, Lüders C, Moehle J, Wallace JW. Seismic design and construction practices for RC structural wall buildings. Earthquake Spectra 2012;28(S1):S245–56.

[4] Massone L, Rojas F. Mw= 8.8 earthquake in Chile, February 27, 2010 (in Spanish). Department of Civil Engineering, University of Chile; 2012.

[5] Taylor C, Cote P, Wallace JW. Design of slender reinforced concrete walls with openings. ACI Struct J 1998;95(4):420–33.

[6] Ali A, Reinforced Wight J. Concrete structural walls with staggered opening configurations under reverse cyclic loading. Report No. UMCE 90–05. Ann Arbor, Michigan: Department of Civil Engineering, University of Michigan; 1990.

[7] Mosoarca M. Failure analysis of RC shear walls with staggered openings under seismic loads. Eng Fail Anal 2014;41:48–64.

[8] Estay C. Characteristics of reinforced concrete walls designed in Chile (in Spanish). Civil Engineering thesis. University of Chile; 2008.

[9] Massone LM, Díaz S, Manríquez I, Rojas F, Herrera R. Experimental cyclic response of RC walls with setback discontinuities. Eng Struct 2019;178:410–422.

[10] Rojas F. Development of a nonlinear quadrilateral layered membrane element with drilling degrees of freedom and a nonlinear quadrilateral thin flat layered shell element for the modeling of reinforced concrete walls PhD Thesis University of Southern California; 2012.

[11] Rojas F, Anderson JC, Massone LM. A nonlinear quadrilateral layered membrane element with drilling degrees of freedom for the modeling of reinforced concrete walls. Eng Struct 2016;124:521–38.

[12] Rojas F, Anderson JC, Massone LM. A nonlinear quadrilateral thin flat layered shell element for the modeling of reinforced concrete wall structures. Bull Earthquake Eng 2018;17(12):6491–6513.

[13] Massone LM, Moroder D. Buckling modeling of reinforcing bars with imperfections. Eng Struct 2009;31:758–67.

